MATEMATIKA, MJIAM, Volume 42, Number 1, 33–48

Elasticity Effects on Hydromagnetic Convective Instability in a Salt Containing Maxwell Nanofluid Saturated Porous Layer

[1]Norazuwin Najihah Mat Tahir* and [2]Seripah Awang Kechil

[1]School of Mathematical Sciences, College of Computing, Informatics and Mathematics, Universiti Teknologi MARA Cawangan Negeri Sembilan, Kampus Seremban, Persiaran Seremban Tiga/1, 70300 Seremban, Negeri Sembilan, Malaysia.
[2]School of Mathematical Sciences, College of Computing, Informatics and Mathematics, Universiti Teknologi MARA, 40450 Shah Alam, Selangor, Malaysia.
*Corresponding author: najihahtahir@uitm.edu.my

Article history
Received: 10 March 2025
Received in revised form: 30 May 2025
Accepted: 19 June 2025
Published on line: 30 April 2026

Abstract Maxwell fluids are important in both theoretical research and practical applications due to their ability to model real-world non-Newtonian behaviors that cannot be captured by simpler Newtonian fluid models. Maxwell fluids provide a realistic and manageable way to study non-Newtonian behavior that are widely applicable across engineering, biology and physics. In essence, Maxwell fluids enabling accurate modelling of materials with memory, where both elastic rebound and viscous flow occur simultaneously. The study examines the double diffusive instability resulting from temperature and nanoparticle concentration gradients. Specifically, it investigates the influence of a magnetic field on convective instabilities in a Maxwell nanofluid saturated porous layer containing salt. Linear stability analysis is utilized to determine the onset of both stationary and oscillatory convection. The Galerkin-type weighted residual method is applied to solve the system analytically. Key parameters examined include the relaxation parameter, solutal Darcy Rayleigh number and Chandrasekhar number. Findings suggest that the magnetic field plays a stabilizing role in both types of convective instability, while the relaxation parameter enhances oscillatory convection. Moreover, the solutal Darcy Rayleigh number contributes to the destabilization of the system in both stationary and oscillatory states. The findings on salt concentration and nanoparticle dynamics can be utilized to enhance targeted drug delivery using magnetic nanoparticles within blood flow.

Keywords Convective instability; Magnetic field; Maxwell nanofluid; Porous; Salt.

Mathematics Subject Classification 76E06, 76A05, 76W05, 76S05.

1 Introduction

The phenomenon of convective instabilities has been extensively explored in fluid mechanics due to its significant implications in engineering and scientific disciplines. Since Pearson [1] foundational theoretical work introduced the Rayleigh number as a primary control parameter,

numerous advancements have been made in the study of thermal instability. Previous research has extensively examined the stability of Marangoni convection by Arifin *et al.* [2] and Kechil *et al.* [3].

Experimental studies have explored heat transfer improvements in non-Newtonian fluids [4], while theoretical research has often modeled nanofluids as Newtonian fluids for instability analyses [5]. However, experimental evidence suggest that the Newtonian framework may not fully capture nanofluid behavior [6]. Although extensive literature covers scenarios assuming uniform boundary conditions for temperature and nanoparticle concentration, there is limited focus on cases involving zero nanoparticle flux. Nield and Kuznetsov [7] introduced modified boundary conditions incorporating thermophoresis effects. Following this, Shivakumara *et al.* [8] investigated convective instability in porous layer saturated with Oldroyd-B type nanofluids, assuming zero nanoparticle volume fraction flux at the boundaries. Tahir *et al.* [9] extended Shivakumara *et al.* [8] work by incorporating magnetic field effects in viscoelastic nanofluids within porous layers. Ruo *et al.* [10] revisited the stability analysis of thermal convection in a porous medium saturated with a nanofluid, as studied by Nield and Kuznetsov [7], by considering the dependence of the thermophoretic diffusion coefficient on the nanoparticle volume fraction.

The Maxwell viscoelastic model is widely recognized for describing stress relaxation. While alternative non-Newtonian fluid models such as the Oldroyd-B, have been explored, the Maxwell model remains fundamental in fluid elasticity studies [11]. Maxwell fluid is viscous in nature, dissipating energy, while also having a significant energy storage capacity that characterizes its elastic response [12, 13]. The modified Darcy-Maxwell is used by Tan and Masuoka [14], Wang and Tan [15]. Yang *et al.* [16], Zhao *et al.* [17, 18] and Gaikwad and Javaji [19] to study the stability analysis of a Maxwell fluid in the porous medium heated from below. They demonstrated that the elasticity of Maxwell fluids has a destabilizing effect on a fluid layer in a porous medium when the relaxation time is increased, which enhances the elasticity of the viscoelastic fluid and lowers the Rayleigh number.

Unfortunately, there are only a few studies on the convection of Maxwell nanofluids. Notably, Umavathi and Mohite [12], as well as Umavathi *et al.* [20], have investigated the stability analysis of a Maxwell nanofluid in a porous medium, if both the temperature and the nanoparticle volume fraction remain constant at the boundaries. The effects of Brownian motion and thermophoresis have been incorporated into a modified Darcy-Maxwell nanofluid model to simulate the momentum equation. However, the present study aims to take a more realistic approach by investigating the double-diffusive instability of a Maxwell nanofluid, assuming that the nanoparticle concentration flux is zero at the boundaries [21, 22].

Magnetic fluid consists of a carrier fluid and a suspension of magnetic particles that exhibit distinct behaviors. As a result, chemical engineering is closely related to and influenced by the effects of a magnetic field on Rayleigh-Benard convection in nanofluids. In addition to previous investigations, a magnetic field can enhance the instability of an initially unstable flow [23]. In the classical Rayleigh-Benard problem of magnetoconvection for a nanofluid layer, the combined effects of thermal buoyancy and the magnetic field lead to a Lorentz force term, which exerts a strong stabilizing influence through the nondimensional parameter known as the Chandrasekhar number. Narayana *et al.* [24] found that the stronger fluid elasticity of a viscoelastic fluid can counteract the stabilizing effect of the magnetic field. Tahir and Kechil [25] expanded on the work of Narayana *et al.* [24] by investigating the effects of an external

magnetic field on convective instabilities in a horizontal viscoelastic nanofluid layer. Recent studies on the stability analysis of mixed convection involving Al2O3/water nanofluid in a porous horizontal channel, under the influence of a magnetic field and thermal radiation, have been conducted by Cedric *et al.* [26].

Meanwhile, Jaimala *et al.* [22] examined the stability of double-diffusive convection in a Darcy porous layer saturated with Maxwell nanofluid in the presence of salt. The enhancement of convective instabilities in a horizontal Maxwell nanofluid, which is of significant practical importance for maximizing oil extraction from underground reservoirs, has been studied by Jaimala *et al.* [22], with consideration given to porosity and the magnetic field. This research builds on previous findings by exploring how external magnetic fields influence convective instabilities in horizontal viscoelastic nanofluid layers containing salt. The combination of zero nanoparticle flux, presence of salt, elasticity and magnetic fields in a study or system is considered a unique contribution in the context of fluid dynamics or transport phenomena, especially in nanofluid research. The unique contribution stems from how the zero nanoparticle flux, salt presence, elasticity and magnetic fields interact to produce nontrivial dynamics in transport processes. Individually, each is significant but together, they represent a rich, underexplored regime in nanofluid research that can provide new theoretical insights and practical engineering solutions. When all four effects are studied simultaneously, the result is a multi-physics, coupled system that reflects highly realistic and complex environments, such as blood flow with nanoparticles and salts under magnetic fields, polymer-based nanofluids used in biomedical or energy applications and cooling flows in magnetic fields with tailored nanofluids for enhanced heat and mass transfer.

2 Methodology

A horizontal porous layer of thickness H, saturated with an incompressible Maxwell nanofluid, is analyzed. The lower boundary is set at $z = 0$ temperature and salt concentration are constant at both boundaries, with no nanoparticle flux. The system is subjected to a uniform vertical magnetic field and equations governing mass, momentum, energy, nanoparticle concentration and salt concentration are formulated. Maxwell's electromagnetic equations for non-Newtonian fluids are incorporated and nondimensionalization is applied to transform the governing equations. Linear stability analysis is performed by introducing perturbations, leading to a system of ordinary differential equations solved using normal mode analysis. The Galerkin-type weighted residual method is employed to obtain critical values of the thermal Darcy-Rayleigh number. The layer is heated and salted from below which the gravity, $\mathbf{g} = -g\hat{\mathbf{e}}_z$ is assumed to act vertically downwards in the presence of a uniform vertical magnetic field $\mathbf{H} = (0, 0, H_0)$. Figure 1 illustrates the schematic diagram of the porous layer.

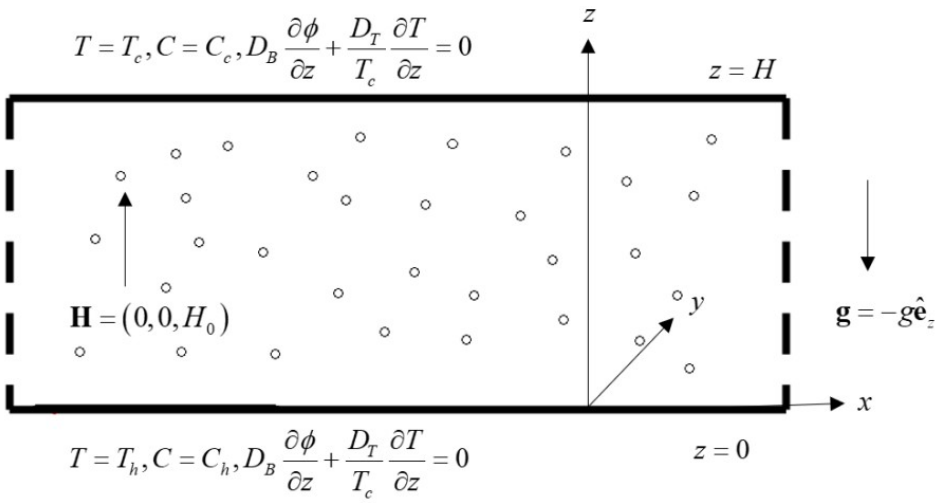

Figure 1: The Schematic Diagram of the Considered Porous Layer

The conservation equations for the mass, momentum, energy, nanoparticle and salt concentration [7,22] are

$$\nabla \cdot \mathbf{q} = 0, \tag{1}$$

$$\frac{\mu}{K}\mathbf{q} = \left(1 + \lambda \frac{\partial}{\partial t}\right) \Bigg\{ -\nabla p + \Big[\phi\rho_p + \rho - \rho\beta_T(T - T_c) - \rho\beta_c(C - C_c) - \phi\rho + \phi\rho\beta_T(T - T_c) + \phi\rho\beta_c(C - C_c)\Big]\mathbf{g} + \frac{\mu_m}{4\pi}(\nabla \times \mathbf{h}) \times \mathbf{H} \Bigg\}, \tag{2}$$

$$(\rho c)_m \frac{\partial T}{\partial t} + (\rho c)_f \mathbf{q} \cdot \nabla T = \kappa_m \nabla^2 T + \varepsilon(\rho c)_p \left[D_B \nabla\phi \cdot \nabla T + \frac{D_T}{T_c} \nabla T \cdot \nabla T \right], \tag{3}$$

$$\frac{\partial \phi}{\partial t} + \frac{1}{\varepsilon}\mathbf{q} \cdot \nabla\phi = D_B \nabla^2 \phi + \frac{D_T}{T_c} \nabla^2 T, \tag{4}$$

$$\frac{\partial C}{\partial t} + \frac{1}{\varepsilon}\mathbf{q} \cdot \nabla C = D_S \nabla^2 C, \tag{5}$$

where $\mathbf{q} = (u, v, w)$ is the velocity vector, μ is the Darcian viscosity, K is the permeability, λ is the relaxation time, t is the time, p is the pressure, ϕ is the nanoparticle volume fraction, ρ is the density of base fluid, ρ_p is the mass density of the nanoparticles, β_T is the volumetric expansion coefficient of the fluid, β_c is the volumetric expansion coefficient of the salt concentration, T is the temperature, C is the salt concentration, T_c is the temperature at the upper surface, C_c

is the concentration of the salt at the upper surface, $\mathbf{g}$ is the acceleration due to gravity, μ_m is the magnetic permeability, $\mathbf{h} = (h_x, h_y, h_z)$ is the components of magnetic field, κ_m is the overall thermal conductivity, ε is the porosity of the porous medium, $(\rho c)_m$, $(\rho c)_p$, $(\rho c)_f$ are the effective heat capacity of the porous medium, nanoparticles and base fluid, respectively, D_B is the Brownian diffusion coefficient, D_T is the thermophoretic diffusion coefficient and D_S is the solute diffusivity.

The Maxwell's electromagnetic equations for non-Newtonian fluid saturated porous layer [27] are

$$\frac{\partial \mathbf{h}}{\partial t} = \frac{1}{\varepsilon}(\mathbf{H} \cdot \nabla)\mathbf{q} + \eta \nabla^2 \mathbf{h}, \tag{6}$$

$$\nabla \cdot \mathbf{h} = 0, \tag{7}$$

where η is the resistivity of the fluid. It is assumed that the lower and upper boundaries maintain a constant temperature and salt concentrations, with no nanoparticle flux [22] given by,

$$w = 0, \frac{\partial w}{\partial z} + a_1 H \frac{\partial^2 w}{\partial z^2} = 0, T = T_h, C = C_h, D_B \frac{\partial \phi}{\partial z} + \frac{D_T}{T_c}\frac{\partial T}{\partial z} = 0 \text{ at } z = 0, \tag{8}$$

$$w = 0, \frac{\partial w}{\partial z} - a_2 H \frac{\partial^2 w}{\partial z^2} = 0, T = T_c, C = C_c, D_B \frac{\partial \phi}{\partial z} + \frac{D_T}{T_c}\frac{\partial T}{\partial z} = 0 \text{ at } z = H, \tag{9}$$

where a_1 and a_2 are constants, T_h is the temperature at the lower surface and C_h is the concentration of salt at the lower surface.

2.1 Nondimensionalization

The system described by equations (1) – (9) will undergo a linear stability analysis to investigate the onset of both stationary and oscillatory instabilities. The introduction of the scaling quantities for the length, velocity, time, nanoparticle volume fraction, temperature, salt concentration, relaxation time, pressure and magnetic field components result in nondimensional variables [22],

$$\begin{aligned}(x^*, y^*, z^*) = \frac{(x, y, z)}{H}, (u^*, v^*, w^*) = \frac{(u, v, w)H}{\alpha_m}, t^* = \frac{t\alpha_m}{MH^2}, \phi^* = \frac{\phi - \phi_0}{\phi_0},\\ T^* = \frac{T - T_c}{T_h - T_c}, C^* = \frac{C - C_c}{C_h - C_c}, \lambda^* = \frac{\lambda H^2}{\alpha_m}, p^* = \frac{pK}{\mu \alpha_m}, \mathbf{h}^* = \frac{\eta}{H_0 \alpha_m}\mathbf{h},\end{aligned} \tag{10}$$

where $\alpha_m = \dfrac{\kappa_m}{(\rho c)_f}$ is the thermal diffusivity of the porous medium, $M = \dfrac{(\rho c)_m}{(\rho c)_f}$ is the heat capacity ratio, and asterisks denote dimensionless quantities. T_c, C_c, and ϕ_0 are the reference

temperature, salt concentration, and nanoparticle concentration, respectively. The dimensionless partial differential equations corresponding to equations (1) – (7) are obtained by applying the scaling quantities (10) and removing the asterisks given by

$$\nabla \cdot \mathbf{q} = 0, \tag{11}$$

$$\mathbf{q} = \left(1 + \frac{\lambda}{M}\frac{\partial}{\partial t}\right)\Bigg\{ -\nabla p - R_m\,\hat{\mathbf{e}}_z - R_n\,\phi\,\hat{\mathbf{e}}_z + R_a\,T\,\hat{\mathbf{e}}_z + \frac{R_s}{L_n}\,C\,\hat{\mathbf{e}}_z + Q\Big[\left(\frac{\partial h_x}{\partial z} - \frac{\partial h_z}{\partial x}\right)\hat{\mathbf{e}}_x - \left(\frac{\partial h_z}{\partial y} - \frac{\partial h_y}{\partial z}\right)\hat{\mathbf{e}}_y\Big]\Bigg\}, \tag{12}$$

$$\frac{\partial T}{\partial t} + \mathbf{q}\cdot\nabla T = \nabla^2 T + \frac{N_B}{L_e}\,\nabla\phi\cdot\nabla T + \frac{N_A N_B}{L_e}\,\nabla T\cdot\nabla T, \tag{13}$$

$$\frac{1}{M}\frac{\partial \phi}{\partial t} + \frac{1}{\varepsilon}\,\mathbf{q}\cdot\nabla\phi = \frac{1}{L_e}\nabla^2\phi + \frac{N_A}{L_e}\nabla^2 T, \tag{14}$$

$$\frac{1}{M}\frac{\partial C}{\partial t} + \frac{1}{\varepsilon}\,\mathbf{q}\cdot\nabla C = \frac{1}{L_n}\nabla^2 C, \tag{15}$$

$$\frac{\varepsilon}{M}\,\frac{P_{r_2}}{P_r}\,\frac{\partial \mathbf{h}}{\partial t} = \left(\frac{\partial u}{\partial z}\,\hat{\mathbf{e}}_x + \frac{\partial v}{\partial z}\,\hat{\mathbf{e}}_y + \frac{\partial w}{\partial z}\,\hat{\mathbf{e}}_z\right) + \varepsilon\nabla^2\mathbf{h}, \tag{16}$$

$$\nabla\cdot\mathbf{h} = 0. \tag{17}$$

Similarly, the corresponding boundary conditions (8)–(9) are transformed into

$$w = 0, \quad \frac{\partial w}{\partial z} + a_1\frac{\partial^2 w}{\partial z^2} = 0, \quad T = 1, \quad C = 1, \quad \frac{\partial \phi}{\partial z} + N_A\frac{\partial T}{\partial z} = 0 \text{ at } z = 0, \tag{18}$$

$$w = 0, \quad \frac{\partial w}{\partial z} - a_2\frac{\partial^2 w}{\partial z^2} = 0, \quad T = 0, \quad C = 0, \quad \frac{\partial \phi}{\partial z} + N_A\frac{\partial T}{\partial z} = 0 \text{ at } z = 1. \tag{19}$$

The following nondimensional parameters [22, 27] are defined

$$\begin{aligned} R_m &= \frac{[\rho_p\phi_0 + \rho(1-\phi_0)]\,gKH}{\mu\alpha_m}, R_n = \frac{(\rho_p - \rho)\phi_0 gKH}{\mu\alpha_m}, \\ R_a &= \frac{\rho g\beta_T KH(T_h - T_c)}{\mu\alpha_m}, R_s = \frac{\rho g\beta_c KH(C_h - C_c)}{\mu D_S}, \\ L_n &= \frac{\alpha_m}{D_S}, \quad Q = \frac{\mu_m H_0^2 K}{4\pi\eta\mu}, \quad N_B = \frac{\varepsilon\phi_0(\rho c)_p}{(\rho c)_f}, \\ N_A &= \frac{D_T(T_h - T_c)}{D_B T_c\phi_0}, Le = \frac{\alpha_m}{D_B}, P_{r_2} = \frac{\mu}{\rho\eta}, P_r = \frac{\mu}{\rho\alpha_m}, \end{aligned} \tag{20}$$

where R_m is the basic density Darcy Rayleigh number, R_n is the concentration Darcy Rayleigh number, R_a is the Darcy Rayleigh number, R_s is the solutal Darcy Rayleigh number, L_n is the thermosolutal Lewis number, Q is the Chandrasekhar number, N_B is the modified particle density increment, N_A is the modified diffusivity ratio, Le is the Lewis number, P_{r_2} is the magnetic Prandtl number, and P_r is the Prandtl number.

2.2 Linear Stability Analysis

When the fluid is stationary, the base quiescent state is described by

$$\mathbf{q} = 0, \quad \mathbf{h} = \mathbf{H}, \quad p = p_b(z), \quad T = T_b(z), \quad \phi = \phi_b(z), \quad C = C_b(z). \tag{21}$$

Substituting (21) into (12) – (15), the basic pressure, temperature, salt concentration and volume fraction of nanoparticles are,

$$\frac{dp_b}{dz} + R_m + R_n\phi_b - R_aT_b - \frac{R_s}{L_n}C_b = 0, \tag{22}$$

$$\frac{d^2T_b}{dz^2} + \frac{N_B}{L_e}\frac{d\phi_b}{dz}\frac{dT_b}{dz} + \frac{N_AN_B}{L_e}\left(\frac{dT_b}{dz}\right)^2 = 0, \tag{23}$$

$$\frac{d^2\phi_b}{dz^2} + N_A\frac{d^2T_b}{dz^2} = 0, \tag{24}$$

$$\frac{d^2C_b}{dz^2} = 0. \tag{25}$$

The zero nanoparticles flux as in boundary conditions (18) and (19) becomes

$$\frac{d\phi_b}{dz} + N_A\frac{dT_b}{dz} = 0. \tag{26}$$

The substitution of (26) in (23) gives,

$$\frac{d^2T_b}{dz^2} = 0. \tag{27}$$

Integrating (27) twice with respect to z and applying the boundary conditions (18) and (19), we obtain

$$T_b = 1 - z. \tag{28}$$

In view of (24) and (26), together with the boundary conditions (18) and (19), the basic nanoparticle concentration and salt concentration are approximated as

$$\phi_b = \phi_0 + N_Az, \tag{29}$$

$$C_b = 1 - z. \tag{30}$$

Integrating (22) using (28)–(30) gives

$$p_b = p_0, \tag{31}$$

where p_0 is the constant reference pressure. The results (28)–(31) are consistent with those derived by Nield and Kuznetsov [7].

2.2.1 Perturbation Solution

The basic state is perturbed by infinitesimal disturbances

$$\mathbf{q} = \mathbf{q}', \quad p = p_b + p', \quad T = T_b + T', \quad \phi = \phi_b + \phi', \quad C = C_b + C', \quad \mathbf{h} = \mathbf{H} + \mathbf{h}', \tag{32}$$

where the prime denotes the perturbation quantity. By applying fundamental calculus and algebraic operations, the linearized perturbed system of equations (11)–(17) becomes

$$\mathbf{q}' = \left(1 + \frac{\lambda}{M}\frac{\partial}{\partial t}\right)\left\{-\nabla p' - R_n\phi'\hat{\mathbf{e}}_z + R_a T'\hat{\mathbf{e}}_z + \frac{R_s}{L_n}C'\hat{\mathbf{e}}_z + Q\Big[\left(\frac{\partial h_x'}{\partial z} - \frac{\partial h_z'}{\partial x}\right)\hat{\mathbf{e}}_x - \left(\frac{\partial h_z'}{\partial y} - \frac{\partial h_y'}{\partial z}\right)\hat{\mathbf{e}}_y\Big]\right\}, \tag{33}$$

$$\frac{\partial T'}{\partial t} - w' = \nabla^2 T' + \frac{N_B}{L_e}\left(N_A\frac{\partial T'}{\partial z} - \frac{\partial \phi'}{\partial z}\right) - \frac{2N_A N_B}{L_e}\frac{\partial T'}{\partial z}, \tag{34}$$

$$\frac{1}{M}\frac{\partial \phi'}{\partial t} + \frac{N_A}{\varepsilon}w' = \frac{1}{L_e}\nabla^2\phi' + \frac{N_A}{L_e}\nabla^2 T', \tag{35}$$

$$\frac{1}{M}\frac{\partial C'}{\partial t} - \frac{1}{\varepsilon}w' = \frac{1}{L_n}\nabla^2 C', \tag{36}$$

$$\frac{\varepsilon}{M}\frac{P_{r_2}}{P_r}\frac{\partial \mathbf{h}'}{\partial t} = \left(\frac{\partial u'}{\partial z}\hat{\mathbf{e}}_x + \frac{\partial v'}{\partial z}\hat{\mathbf{e}}_y + \frac{\partial w'}{\partial z}\hat{\mathbf{e}}_z\right) + \varepsilon\nabla^2\mathbf{h}', \tag{37}$$

$$\nabla \cdot \mathbf{h}' = 0, \tag{38}$$

where ∇^2 is the three-dimensional Laplacian operator. The boundary conditions (18) and (19) become

$$w' = 0, \quad \frac{\partial w'}{\partial z} + a_1\frac{\partial^2 w'}{\partial z^2} = 0, \quad T' = 0, \quad C' = 0, \quad \frac{\partial \phi'}{\partial z} + N_A\frac{\partial T'}{\partial z} = 0 \text{ at } z = 0, \tag{39}$$

$$w' = 0, \quad \frac{\partial w'}{\partial z} - a_2\frac{\partial^2 w'}{\partial z^2} = 0, \quad T' = 0, \quad C' = 0, \quad \frac{\partial \phi'}{\partial z} + N_A\frac{\partial T'}{\partial z} = 0 \text{ at } z = 1. \tag{40}$$

Applying the curl operator twice to the momentum equation (33) and substituting the pressure term (22), the momentum equation (33) simplifies to

$$\nabla^2 w' + \left(1 + \frac{\lambda}{M}\frac{\partial}{\partial t}\right)\left(\nabla_H^2 R_n\phi' - \nabla_H^2 R_a T' - \nabla_H^2\frac{R_s}{L_n}C' - Q\nabla^2\frac{\partial h_z'}{\partial z}\right) = 0, \tag{41}$$

where ∇_H^2 is the two-dimensional Laplacian operator in the horizontal plane. Following Gupta et al [27], we introduce the vorticity and current density as $\varsigma = \dfrac{\partial v'}{\partial x} - \dfrac{\partial u'}{\partial y}$ and $\xi = \dfrac{\partial h_y'}{\partial x} - \dfrac{\partial h_x'}{\partial y}$, respectively and hence, equations (33), (37) and (38) are transformed into

$$\varsigma = \left(1 + \frac{\lambda}{M}\frac{\partial}{\partial t}\right) Q\frac{\partial \xi}{\partial z}, \tag{42}$$

$$\frac{\varepsilon}{M}\frac{P_{r_2}}{P_r}\frac{\partial \xi}{\partial t} = \frac{\partial \varsigma}{\partial z} + \varepsilon \nabla^2 \xi, \tag{43}$$

$$\frac{\varepsilon}{M}\frac{P_{r_2}}{P_r}\frac{\partial h_z'}{\partial t} - \varepsilon \nabla^2 h_z' = \frac{\partial w'}{\partial z}. \tag{44}$$

2.2.2 Normal Modes

The partial differential equations (34)–(36), (41)–(44), along with the boundary conditions in (39) and (40), form a linear boundary-value problem that can be converted into a system of ordinary differential equations using the method of normal modes. The superposition of normal modes in the form of two-dimensional periodic waves is given by

$$(w', T', C', \phi', h_z', \xi, \varsigma) = [W(z), \Theta(z), \eta(z), \Phi(z), K(z), X(z), Z(z)]e^{(st + i\alpha_x + i\alpha_y)}, \tag{45}$$

where $W(z), \Theta(z), \eta(z), \Phi(z), K(z), X(z)$ and $Z(z)$ are the amplitudes of the velocity, temperature, salt, nanoparticle volume fraction, magnetic field, current density and vorticity, respectively. The total wave number is $\alpha = (\alpha_x^2 + \alpha_y^2)^{1/2}$ and $s = s_r + is_i$ is a dimensionless complex growth rate, where $\mathrm{Re}(s) = s_r$ is the growth rate and $\mathrm{Im}(s) = s_i$ is the frequency. For neutral stability, $s_r = 0$. Stationary convection occurs when $s_i = 0$, otherwise the convection is oscillatory when $s_i \neq 0$.

The system (41)–(44) and (34)–(36) in terms of normal modes is expressed as

$$(D^2 - \alpha^2)W + \left(1 + \frac{\lambda}{M}s\right)\left[-R_n\alpha^2\Phi + R_a\alpha^2\Theta + \frac{R_s}{L_n}\alpha^2\eta - Q(D^2 - \alpha^2)DK\right] = 0, \tag{46}$$

$$Z = \left(1 + \frac{\lambda}{M}s\right) QDX, \tag{47}$$

$$\left[\frac{\varepsilon}{M}\frac{P_{r_2}}{P_r}s - \varepsilon(D^2 - \alpha^2)\right] X = DZ, \tag{48}$$

$$\left[\frac{\varepsilon}{M}\frac{P_{r_2}}{P_r}s - \varepsilon(D^2 - \alpha^2)\right] K = DW, \tag{49}$$

$$W + \left(D^2 - \alpha^2 - \frac{N_A N_B}{Le}D - s\right)\Theta - \frac{N_B}{Le}D\Phi = 0, \tag{50}$$

$$\frac{W}{\varepsilon} + \left[\frac{1}{L_n}(D^2 - \alpha^2) - \frac{s}{M}\right]\eta = 0, \tag{51}$$

$$\frac{N_A}{\varepsilon}W - \frac{N_A}{Le}(D^2 - \alpha^2)\Theta - \left[\frac{1}{Le}(D^2 - \alpha^2) - \frac{s}{M}\right]\Phi = 0, \tag{52}$$

where $D \equiv \dfrac{d}{dz}$. The corresponding boundary conditions become

$$W = 0, \quad DW + a_1 D^2 W = 0, \quad \Theta = 0, \quad \eta = 0, \quad D\Phi + N_A D\Theta = 0 \text{ at } z = 0, \tag{53}$$

$$W = 0, \quad DW - a_2 D^2 W = 0, \quad \Theta = 0, \quad \eta = 0, \quad D\Phi + N_A D\Theta = 0 \text{ at } z = 1. \tag{54}$$

The case with free lower and upper boundaries is considered. For free lower and upper boundaries at $z = 0$ and $z = 1$, the boundary conditions reduce to

$$W = 0, \quad D^2 W = 0, \quad \Theta = 0, \quad \eta = 0, \quad D\Phi + N_A D\Theta = 0. \tag{55}$$

Substituting K from (49) into (46), we obtain

$$\left[\frac{\varepsilon}{M}\frac{P_{r_2}}{P_r}(D^2 - \alpha^2) - \varepsilon(D^2 - \alpha^2)^2 - \left(1 + \frac{\lambda}{M}s\right) QD^2(D^2 - \alpha^2)\right] W + \alpha^2 \left(1 + \frac{\lambda}{M}s\right)\left[\frac{\varepsilon}{M}\frac{P_{r_2}}{P_r} - \varepsilon(D^2 - \alpha^2)\right]\left(-R_n\Phi + R_a\Theta + \frac{R_s}{L_n}\eta\right) = 0. \tag{56}$$

The Galerkin-type weighted residual method is used to approximate the closed-form solution of the system (50)–(52) and (56), with boundary condition (55). In the method of Galerkin-type weighted residuals, the functions W, Θ, η, and Φ are expressed as

$$W = \sum_{n=1}^{N} A_n W_n, \quad \Theta = \sum_{n=1}^{N} B_n \Theta_n, \quad \eta = \sum_{n=1}^{N} C_n \eta_n, \quad \Phi = \sum_{n=1}^{N} D_n \Phi_n, \tag{57}$$

where A_n, B_n, C_n, and D_n are unknown coefficients with $n = 1, 2, 3, \cdots, N$. Equations (50)–(52) and (56) are multiplied, respectively, by Θ, η, Φ and W, as in (57). For free-free boundaries, the trial functions are

$$W_1 = \Theta_1 = \eta_1 = \sin(\pi z), \quad \Phi_1 = -N_A \sin(\pi z), \tag{58}$$

where W_1, Θ_1, η_1 and Φ_1 are trial functions that satisfy the boundary conditions (55).

3 Results and Discussions

The key critical parameter is the thermal Darcy Rayleigh number, R_a, which determines the onset of instability. The complex growth rate s is set to $s = i\omega$; for stationary convection $\omega = 0$, and for oscillatory convection, $\omega \neq 0$. The thermal Darcy Rayleigh number has a nontrivial solution that can be obtained using the Galerkin-type weighted residuals, given by

$$R_a = \frac{J + i\omega}{\varepsilon\alpha^2}\left(\frac{M}{M + \lambda i\omega}\right)\left(\frac{MP_r}{JMP_r + P_{r_2} i\omega}\right)\left\{\left[\frac{\varepsilon}{M}\frac{P_{r_2}}{P_r} i\omega + 2\varepsilon\alpha^2 + \left(1 + \frac{\lambda}{M} i\omega\right) Q\alpha^2\right]\pi^2 + \left[\varepsilon + \left(1 + \frac{\lambda}{M} i\omega\right) Q\right]\pi^4 + \frac{\varepsilon}{M}\frac{P_{r_2}}{P_r}\alpha^2 i\omega + \varepsilon\alpha^4\right\} - N_A R_n \left(\frac{LeJ + \varepsilon J + i\omega Le}{\varepsilon}\right)\left(\frac{M}{MJ + i\omega Le}\right) - R_s\left(\frac{M}{MJ + i\omega L_n}\right)\left(\frac{J + i\omega}{\varepsilon}\right), \tag{59}$$

where $J = \pi^2 + \alpha^2$. The modified particle density increment, N_B, does not appear, while the modified diffusivity ratio, N_A, appears only in relation to the concentration Darcy Rayleigh number, R_n. In this approximation, the nanofluid cross-diffusion terms are dominated by the regular cross-diffusion term [5]. The thermal Darcy Rayleigh number in its complex form, along with its real and imaginary parts, is given by

$$\begin{aligned} R_{a_R} = &\left[\frac{M^2P_r\left(JMP_r(JM+\lambda\omega^2)+\omega^2P_{r_2}(-J\lambda+M)\right)}{\varepsilon\alpha^2\left(J^2M^2P_r^2+\omega^2P_r^2\right)\left(M^2+\lambda^2\omega^2\right)}\right](\varepsilon J^2+Q\pi^2J) \\ &-\omega^2J\left(\frac{\varepsilon}{M}\frac{P_{r_2}}{P_r}+\frac{\lambda}{M}Q\pi^2\right)\left[\frac{M^2P_r\left(JMP_r(-J\lambda+M)+P_{r_2}(JM+\lambda\omega^2)\right)}{\varepsilon\alpha^2\left(J^2M^2P_r^2+\omega^2P_r^2\right)\left(M^2+\lambda^2\omega^2\right)}\right] \\ &-\frac{R_sM}{\varepsilon}\left(\frac{MJ^2+L_n\omega^2}{M^2J^2+L_n^2\omega^2}\right)-\frac{N_AR_nM}{\varepsilon}\left[\frac{MJ^2(Le+\varepsilon)+Le^2\omega^2}{M^2J^2+Le^2\omega^2}\right], \end{aligned} \tag{60}$$

and

$$\begin{aligned} R_{a_i} = &\left[\frac{M^2P_r\left(JMP_r(JM+\lambda\omega^2)+\omega^2P_{r_2}(-J\lambda+M)\right)}{\varepsilon\alpha^2\left(J^2M^2P_r^2+\omega^2P_{r_2}^2\right)\left(M^2+\lambda^2\omega^2\right)}\right]\left(\frac{\varepsilon}{M}\frac{P_{r_2}}{P_r}+\frac{\lambda}{M}Q\pi^2\right)J\omega \\ &-\omega(\varepsilon J^2+Q\pi^2J)\left[\frac{M^2P_r\left(JMP_r(-J\lambda+M)+P_{r_2}(JM+\lambda\omega^2)\right)}{\varepsilon\alpha^2\left(J^2M^2P_r^2+\omega^2P_{r_2}^2\right)\left(M^2+\lambda^2\omega^2\right)}\right] \\ &-\frac{R_s}{\varepsilon}\left(\frac{-JML_n+M^2J}{M^2J^2+L_n^2\omega^2}\right)\omega-\frac{N_AR_n}{\varepsilon}\left(\frac{M-Le-\varepsilon}{M^2J^2+Le^2\omega^2}\right)MJLe\omega. \end{aligned} \tag{61}$$

3.1 Stationary Convection

The result for the stationary convection ($\omega = 0$) is

$$R_{a\text{stat}} = \frac{J^2}{\alpha^2}+\frac{Q\pi^2J}{\varepsilon\alpha^2}-N_AR_n\left(1+\frac{\text{Le}}{\varepsilon}\right)-\frac{R_s}{\varepsilon}. \tag{62}$$

In the absence of magnetic field $Q = 0$, equation (62) reduces to the solution obtained by Jaimala *et al.* [22] for stationary convection.

3.2 Oscillatory Convection

Setting $R_{a_i} = 0$ gives the corresponding value of ω for the onset of oscillatory convection. The solution for the oscillatory convection is

$$\begin{aligned} R_{a_{\text{osc}}} = &\left[\frac{M^2P_r\left(JMP_r(JM+\lambda\omega^2)+\omega^2P_{r_2}(-J\lambda+M)\right)}{\varepsilon\alpha^2\left(J^2M^2P_r^2+\omega^2P_{r_2}^2\right)\left(M^2+\lambda^2\omega^2\right)}\right](\varepsilon J^2+Q\pi^2J) \\ &-\omega^2J\left(\frac{\varepsilon}{M}\frac{P_{r_2}}{P_r}+\frac{\lambda}{M}Q\pi^2\right)\left[\frac{M^2P_r\left(JMP_r(-J\lambda+M)-P_{r_2}(JM+\lambda\omega^2)\right)}{\varepsilon\alpha^2\left(J^2M^2P_r^2+\omega^2P_{r_2}^2\right)\left(M^2+\lambda^2\omega^2\right)}\right] \\ &-\frac{R_sM}{\varepsilon}\left(\frac{MJ^2+L_n\omega^2}{M^2J^2+L_n^2\omega^2}\right)-\frac{N_AR_nM}{\varepsilon}\left(\frac{MJ^2(Le+\varepsilon)+Le^2\omega^2}{M^2J^2+Le^2\omega^2}\right). \end{aligned} \tag{63}$$

The stability curves of the thermal Darcy Rayleigh number are plotted in the (α, R_a) plane. The effect of the relaxation parameter λ is illustrated in Figure 2. The stationary instability is independent of the relaxation parameter. A fluid relaxation time λ is defined to quantify the viscoelastic behavior based on the Maxwell fluid model theory [28]. It is observed that the oscillatory thermal Darcy Rayleigh number decreases as the relaxation parameter increases. An increase in the relaxation parameter enhances the elasticity of the Maxwell fluid, which has a destabilizing effect on the fluid layer in the porous media.

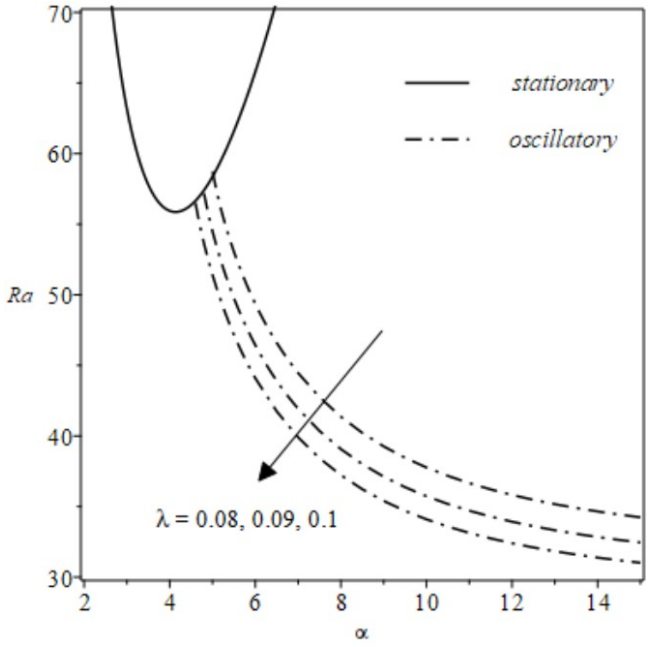

Figure 2: Stability curves of convection for various values of the relaxation parameter λ, given $R_n = 0.4$, $R_s = 0.5$, $Le = 10$, $\varepsilon = 0.5$, $L_n = 10$, $N_A = 2$, $M = 1.1$, $Q = 1$, $P_r = 1.0$, and $P_{r_2} = 0.01$.

Furthermore, Figure 3 displays the stability curves for stationary and oscillatory convection, showing the variations of the thermal Darcy Rayleigh number as a function of the wave number, α for different values of the solutal Darcy Rayleigh number. The solute concentration exceeds that of the solvent, leading to a decrease in both the stationary and oscillatory thermal Darcy Rayleigh numbers. As a result, the system becomes unstable in the Maxwell nanofluid layer. This is consistent with the result obtained by Jaimala *et al.* [22] in the absence of a magnetic field.

Meanwhile, Figure 4 illustrates the variation of the stationary and oscillatory thermal Darcy Rayleigh numbers for different values of the Chandrasekhar number. A significant increase in both the stationary and oscillatory thermal Darcy Rayleigh numbers is observed with an increase in the Chandrasekhar number. The increase in the magnetic parameter indicates a stronger Lorentz force, which produces viscous drag and causes a reduction in the fluid velocity. As a result, the magnetic field stabilizes the nanofluid layer and the stabilizing effect becomes more pronounced with a stronger magnetic field. The magnetic field imparts rigidity and elasticity to the fluid, which are crucial factors influencing its stability.

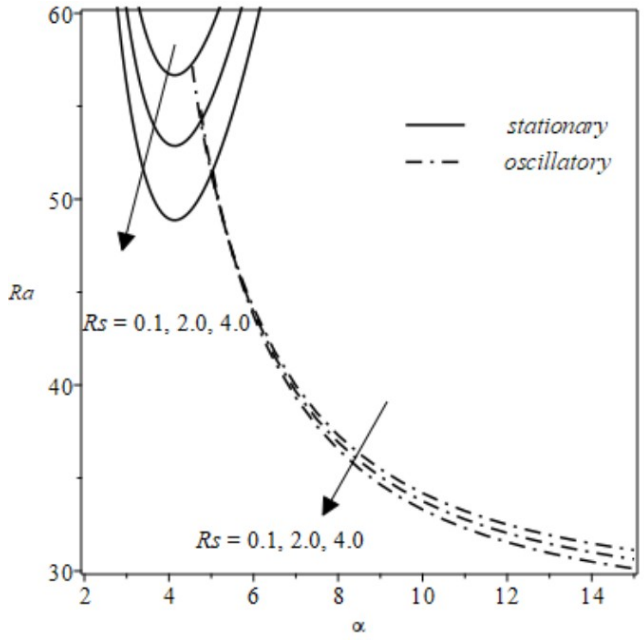

Figure 3: Stability curves of convection for various values of the solutal Darcy Rayleigh number R_s, given $R_n = 0.4$, $Le = 10$, $N_A = 2$, $\varepsilon = 0.5$, $L_n = 10$, $M = 1.1$, $\lambda = 0.1$, $Q = 1$, $P_r = 1.0$, and $P_{r_2} = 0.01$.

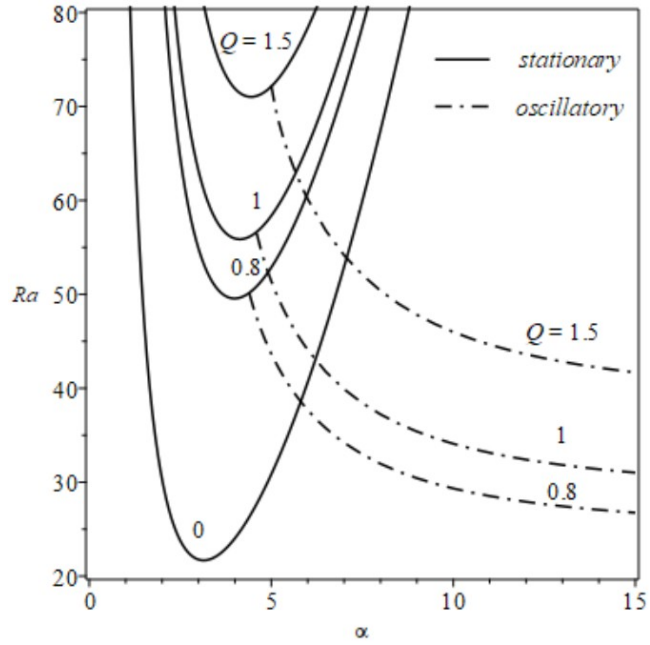

Figure 4: Stability curves of convection for various values of the Chandrasekhar number Q, given $R_n = 0.4$, $R_s = 0.5$, $Le = 10$, $\varepsilon = 0.5$, $L_n = 10$, $N_A = 2$, $M = 1.1$, $\lambda = 0.1$, $P_r = 1.0$, and $P_{r_2} = 0.01$.

4 Conclusion

This study analytically investigates the impact of stress relaxation, solutal Darcy Rayleigh number and magnetic field on convective instabilities in Maxwell nanofluid saturated porous layers. Results indicate that the solutal Darcy Rayleigh number enhances instability, while the relaxation parameter destabilizes oscillatory convection. The relaxation parameter introduces time delayed elastic effects. Meanwhile, the magnetic field stabilizes the system by exerting a strong Lorentz force. The magnetic field introduces instantaneous damping forces which can be applied to control flow, reduce defects and enhance heat transfer during manufacturing. Together, relaxation parameter and magnetic field can create a complex interplay such as elastic memory wants to keep moving and magnetic damping tries to stop the motion. The result is a flow that might oscillate, slow down or even stiffen depending on the strength of each effect. These findings contribute to a better understanding of hydromagnetic convective instability, particularly applicable to multiple real-world systems in engineering, biomedicine and environmental science. The results of salt concentration and nanoparticle dynamics can be applied in targeted drug delivery using magnetic nanoparticles in blood flow.

Acknowledgments

The authors appreciate the support provided by Universiti Teknologi MARA (UITM) for this study.

References

[1] Pearson, J. R. A. On convection cells induced by surface tension, *Journal of Fluid Mechanics*, 4(5) (1958), 489–500. https://doi.org/10.1017/S0022112058000616

[2] Mokhtar, N. F. M., Arifin, N. M., Nazar, R., Ismail, F. and Suleiman, M. Effect of internal heat generation on Marangoni convection in a superposed fluid-porous layer with deformable free surface, *International Journal of Physical Sciences*, 6(23) (2011), 5550–5563.

[3] Kechil, S. A. and Allias, R. Steady Marangoni instabilities in variable-viscosity liquid layer in the presence of insoluble surfactant, *Journal of Physics: Conference Series*, 1770(1) (2021), 012044. https://doi.org/10.1088/1742-6596/1770/1/012044

[4] Ling, Z., He, Z., Xu, T., Fang, X., Gao, X. and Zhang, Z. Experimental and numerical investigation on non-Newtonian nanofluids flowing in shell side of helical baffled heat exchanger combined with elliptic tubes, *Applied Sciences*, 7(1) (2017), 48. https://doi.org/10.3390/app7010048

[5] Chand, R., Rana, G. C. and Yadav, D. Thermal instability in a layer of couple stress nanofluid saturated porous medium, *Journal of Theoretical and Applied Mechanics*, 47(1) (2017), 69. https://doi.org/10.1515/jtam-2017-0005

[6] Sun, M. H., Wang, G. B. and Zhang, X. R. Rayleigh–Bénard convection of non-Newtonian nanofluids considering Brownian motion and thermophoresis, *International Journal of*

Thermal Sciences, 139 (2019), 312–325. https://doi.org/10.1016/j.ijthermalsci.2019.02.007

[7] Nield, D. A. and Kuznetsov, A. V. Thermal instability in a porous medium layer saturated by a nanofluid: A revised model, *International Journal of Heat and Mass Transfer*, 52 (2009), 5796–5801. https://doi.org/10.1016/j.ijheatmasstransfer.2013.09.026

[8] Shivakumara, I. S., Dhananjaya, M. and Ng, C. O. Thermal convective instability in an Oldroyd-B nanofluid saturated porous layer, *International Journal of Heat and Mass Transfer*, 84 (2015), 167–177. https://doi.org/10.1016/j.ijheatmasstransfer.2015.01.010

[9] Tahir, N. N. M., Ishak, F. and Kechil, S. A. Magneto-convective instability in a horizontal viscoelastic nanofluid saturated porous layer, *Jurnal Teknologi*, 78 (2016), 12–13. https://doi.org/10.11113/jt.v78.10038

[10] Ruo, A. C., Yan, W. M., Chang, M. H. and Yang, T. F. Thermal instability of a horizontal nanofluid layer in a porous medium with high porosity, *Journal of Mechanics*, 38 (2022), 643–658. https://doi.org/10.1093/jom/ufac049

[11] Chen, Y. and Zhu, Y. Global well-posedness of 2D incompressible Oldroyd-B model with only velocity dissipation, *Journal of Differential Equations*, 376 (2023), 606–632. https://doi.org/10.1016/j.jde.2023.09.014

[12] Umavathi, J. C. and Mohite, M. B. Convective transport in a porous medium layer saturated with a Maxwell nanofluid, *Journal of King Saud University – Engineering Sciences*, 28(1) (2016), 56–68. https://doi.org/10.1016/j.jksues.2014.01.002

[13] Zhang, X. H., Shah, R., Saleem, S., Shah, N. A., Khan, Z. A. and Chung, J. D. Natural convection flow Maxwell fluids with generalized thermal transport and Newtonian heating, *Case Studies in Thermal Engineering*, 27 (2021), 101226. https://doi.org/10.1016/j.csite.2021.101226

[14] Tan, W. and Masuoka, T. Stability analysis of a Maxwell fluid in a porous medium heated from below, *Physics Letters A*, 360(3) (2007), 454–460. https://doi.org/10.1016/j.physleta.2006.08.054

[15] Wang, S. and Tan, W. Stability analysis of double-diffusive convection of Maxwell fluid in a porous medium heated from below, *Physics Letters A*, 372(17) (2008), 3046–3050. https://doi.org/10.1016/j.physleta.2008.01.024

[16] Yang, Z., Wang, S., Zhao, M., Li, S. and Zhang, Q. The onset of double diffusive convection in a viscoelastic fluid saturated porous layer with non-equilibrium model, *PLoS One*, 8(11) (2013), e79956. https://doi.org/10.1371/journal.pone.0079956

[17] Zhao, M., Zhang, Q. and Wang, S. Onset of triply diffusive convection in a Maxwell fluid saturated porous layer, *Applied Mathematical Modelling*, 38(9–10) (2014), 2345–2352.

[18] Zhao, M., Zhang, Q. and Wang, S. Linear and nonlinear stability analysis of double diffusive convection in a Maxwell fluid saturated porous layer with internal heat source, *Journal of Applied Mathematics*, 2014 (2014). https://doi.org/10.1155/2014/489279

[19] Gaikwad, S. N. and Javaji, A. V. Onset of Darcy–Brinkman convection in a Maxwell fluid saturated anisotropic porous layer, *Journal of Applied Fluid Mechanics*, 9(4) (2016), 1709–1720.

[20] Umavathi, J. C., Yadav, D. and Mohite, M. B. Linear and nonlinear stability analysis of double-diffusive convection in a porous medium layer saturated in a Maxwell nanofluid with variable viscosity and conductivity, *Elixir Mechanical Engineering*, 79 (2015), 30407–30426.

[21] Jaimala, B., Singh, R. A. and Tyagi, V. K. A macroscopic filtration model for natural convection in a Darcy Maxwell nanofluid saturated porous layer with no nanoparticle flux at the boundary, *International Journal of Heat and Mass Transfer*, 111 (2017), 451–466. https://doi.org/10.1016/j.ijheatmasstransfer.2017.04.003

[22] Jaimala, B., Singh, R. A. and Tyagi, V. K. Stability of double diffusive convection in a Darcy porous layer saturated with Maxwell nanofluid under macroscopic filtration, *International Journal of Heat and Mass Transfer*, 125 (2018), 290–309. https://doi.org/10.1016/j.ijheatmasstransfer.2018.04.070

[23] Yang, Z., Hussain, Z., Hussanan, A., Hussain, S. and Zhang, H. Instability of magnetohydrodynamic flow of Hartmann layers between parallel plates, *AIP Advances*, 9(5) (2019), 055003. https://doi.org/10.1063/1.5086975

[24] Narayana, M., Gaikwad, S. N., Sibanda, P. and Malge, R. Double diffusive magneto-convection in viscoelastic fluids, *International Journal of Heat and Mass Transfer*, 67 (2013), 194–201. https://doi.org/10.1016/j.ijheatmasstransfer.2013.08.027

[25] Tahir, N. N. M. and Kechil, S. A. Elasticity effects on hydromagnetic convective instability in viscoelastic nanofluid layer, *ASM Science Journal*, (2019), 87–93.

[26] Cedric, G. N. K., Pascalin, T. K., Didier, F. and Ghislain, T. Stability analysis of mixed convection in a porous horizontal channel filled with a Newtonian Al_2O_3/water nanofluid in the presence of magnetic field and thermal radiation, *Chinese Journal of Physics*, 79(7) (2022), 514–530. https://doi.org/10.1016/j.cjph.2022.08.024

[27] Gupta, U., Ahuja, J. and Wanchoo, R. K. Magneto convection in a nanofluid layer, *International Journal of Heat and Mass Transfer*, 64 (2013), 1163–1171. https://doi.org/10.1016/j.ijheatmasstransfer.2013.05.035

[28] Chhabra, R. P. and Richardson, J. F. *Non-Newtonian Flow in the Process Industries: Fundamentals and Engineering Applications*, Butterworth-Heinemann, 1999. https://doi.org/10.1002/cjce.5450790324